

State-Of-Charge evaluation of supercapacitors

M. Ceraolo¹, G. Lutzemberger¹, D. Poli¹

¹ Department of Energy, Systems, Territory and Constructions Engineering, University of Pisa,
Largo Lucio Lazzarino n. 1, 56122, Pisa (Italy)

*Corresponding author: tel. +39 050 2217311,
email: lutzemberger@dsea.unipi.it

Abstract

In the last years, energy storage systems are increasingly involved in applications in which they are required to deliver or adsorb significant charging or discharging currents in short intervals of time, typically a few seconds. Thanks to their high specific power, supercapacitors may represent one of the most promising technologies for this kind of applications. However, one of the main concerns regarding their operation is the accurate estimation of their state of charge; the most common technique, based on ampere-hour counting, typically requires some correction mechanisms, since it implies a significant loss of accuracy over time, due to the accumulation of measuring errors.

In the present paper, a novel algorithm to assess the state of charge of supercapacitors is described and implemented. The algorithm is based on the evaluation of the parameters of an equivalent electric circuit of the supercapacitor, and on the consequent use of a Luenberger-style technique for the runtime evaluation of its state of charge, based on the measure of current and voltage at supercapacitor's terminals. The algorithm estimates the cell open circuit voltage while the current is highly variable, as typical in power-oriented applications, hence the corresponding state of charge.

Keywords: Luenberger-style technique; power-oriented application; runtime evaluation; state of charge; supercapacitors.

1 Introduction

Energy storage systems are increasingly required to deliver or adsorb very high currents in short intervals of time, typically few seconds or tens of seconds. This kind of performance is commonly described saying that the considered storage device is “power oriented”. Several case studies may be cited. As an example, hybrid vehicles are moved by at least two energy sources, one of them fuel-powered, the other composed by a storage system. Typically, as described in [1] [2] [3], the first meets the average load, while the storage system delivers or absorbs the ripple around the average value of requested power, thus providing energy during acceleration, while recovering energy during braking. Usually, acceleration and braking phases last seconds or, at most, tens of seconds, thus requiring high currents.

Another case study of interest is oriented to railway applications, in which there is the need to recover braking energy of trams or trains. Several studies have investigated tramway systems [4] [5] [6]. Depending on the considered case study, the energy storage system provides current peaks for about 10-20 s.

One of the most promising technology for this kind of applications is constituted by supercapacitors (SCs), typically characterised by high power and low energy density. Furthermore, due to the absence of electrochemical reactions during charging and discharging processes, supercapacitors are also suitable for workloads characterised by hundreds of thousands charging and discharging cycles, without significant aging phenomena, and very fast dynamic, up to some Hz. However it's worth noticing that in some applications modern high power lithium batteries could be just as competitive and effective, as demonstrated in [7][8][9].

One of the most pressing concerns of designers and users of supercapacitors is how accurately assess the state of charge (SOC) of the energy storage system. The easiest technique is to evaluate SOC based on ampere-hour counting, i.e. integrating the current at the supercapacitor's terminals. Nevertheless, if specific correction mechanisms are not adopted, the accuracy of this technique is jeopardized by the accumulation over time of unavoidable measuring errors.

The most common technique to correct this drift is the so-called OCV-SOC correlation, which requires the supercapacitor's current to be kept at zero for a while; at the end of this phase, the voltage measured at capacitor's terminals corresponds to the open circuit voltage (OCV) of the supercapacitor. The need for a

time interval in which the current is null is however a clear disadvantage of this technique, especially in power oriented applications, in which the current typically varies continuously over time.

This paper is aimed to show and discuss a novel algorithm for the evaluation of the state of charge (SOC) of a supercapacitor, even during transients with highly variable currents. The existing scientific literature significantly lacks about this topic. In fact, most of the literature about supercapacitors is focused on the evaluation of their performance, investigates aging phenomena [10] [11] or analyzes technical improvements like the use of new materials for electrolytes [12] or electrodes [13]. Contrary to the case of batteries, very few studies are focused on supercapacitors' SOC evaluation; a technique based on a Kalman filter is for instance proposed in [14].

The possibility of adapting to supercapacitors some SOC evaluation algorithms widely tested and used for batteries is far from obvious; in fact, in the case of supercapacitors, currents are significantly higher, so the errors due to current integration are a major concern. In particular, the Luenberger-style algorithm described in [15] for the SOC estimation of batteries was never adapted to be implemented and tested on SCs.

In order to assess if a SOC estimation algorithm originally deployed for batteries may be used also for SCs and how effectively it works, it's worth remembering that these techniques require the formulation of proper mathematical models. The accurate identification of the model's numerical parameters on real case studies, the right setup of the SOC estimation algorithm, and the experimental validation of the quality of both the model and SOC estimation algorithm are described in the following. Since the model's numerical parameters may depend on SOC itself, a discussion about the definition of SOC is also reported in the section that describes the model formulation. Assuming a realistic case study, the SOC estimation problem is firstly approached with an Ampere-hour counting technique, with the simple addition of a voltage-based compensation; subsequently, the Luenberger-style technique is implemented, compared and experimentally validated.

2 Model formulation

2.1 Equivalent circuit representation

The models of SCs described in the literature are usually based on an equivalent electric circuit able to represent the voltage/current profile when a current/voltage profile is imposed to its terminals. Two general approaches are commonly followed: the first one is based on a time-domain analysis [16]-[19], validated by experimental laboratory tests [20] or in real existing applications [21]. The second one is performed in the frequency domain [22]-[24].

Both approaches show a general uniformity of models, basically based on the equivalent circuit depicted in Figure 1 [22]. This general model is able to fully represent the dynamic behavior of the device. Furthermore, it is described by a small number of independent parameters, easy to be determined.

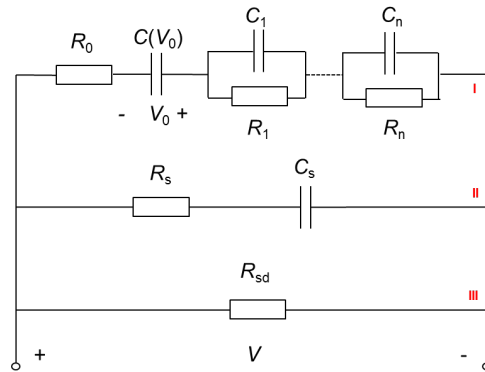


Figure 1: General model of a SC

The model shown in the previous figure is composed by three branches:

- The first branch consists of the series connection of the resistance R_0 , of the main non-linear capacitance $C(V_0)$, and of n parallel R-C blocks; this branch accounts for the frequency response of the device in the frequencies ranging from 10^{-2} to 10^3 Hz.
- The second branch consists of the series connection of the resistance R_s and the capacitance C_s ; it represents the dynamics of the device for frequencies between 10^{-3} and 10^{-6} Hz, corresponding to the redistribution of the electric charges on the electrolytic solution.

- The R_{sd} branch takes into account the self-discharge of the device, whose effect becomes evident for frequencies below 10^{-6} Hz.

If the slow dynamics of the device is not under investigation, the second and the third branches of the model can be neglected [22]. This latter configuration, characterised by the presence of a single branch with a generic number of R-C blocks, is reported in Figure 2. It must be observed that, as specified before, this approach is normally considered also for batteries [25] [26]. According to this model, the voltage across the main capacitance is V_{OC} , also commonly named OCV (Open Circuit Voltage), which corresponds to the voltage that appears at the supercapacitor's terminals after transients settle down.

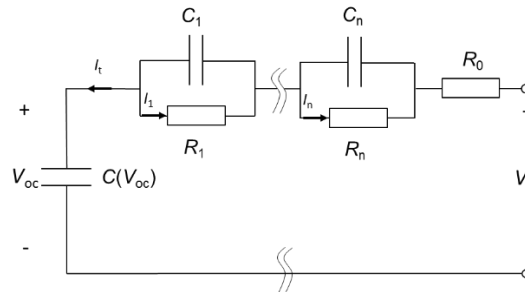


Figure 2: Selected model for SC

The number n of R-C blocks has to be chosen as a compromise between the ease to use (lower values) and the desired accuracy (higher values). In order to avoid excessive complexity of the model and of the procedure required to evaluate the numerical values of model's parameters, it is normally assumed $n=1$ or $n=2$.

Since the transients simulated by the R-C blocks have time constants around one or tens of seconds, whenever only the very first part of the capacitor's dynamic response is of interest, $n=0$ can be assumed. In this case, the first branch is simply composed by the capacitance $C(V_{OC})$ with the resistor R_0 . Naturally, the correspondent precision is expected to be low, but also the procedure to obtain the parameters from experimental tests is simplified. Finally, although some papers show that the dependence of C on V_{OC} is not negligible [27], often a constant value of C is typically assumed.

2.2 SOC definition

The State-Of-Charge (SOC) is very commonly used in electrochemical batteries as an indicator of the level of charge stored into the device: it is assumed to be 1 and 0, respectively when the battery is fully charged and totally discharged. This indicator is also commonly used for supercapacitors, although its definitions are not always perfectly corresponding. For instance, in [28] [29] the following definitions (1a) and (1b) are used, respectively:

$SOC_{er} = \frac{V_{OC}^2 - V_{min}^2}{V_{max}^2 - V_{min}^2}$	(1a)
$SOC_{qr} = \frac{V_{OC} - V_{min}}{V_{max} - V_{min}}$	(1b)

The first definition, SOC_{er} , associates the SOC to the supercapacitor's energy content (which is reflected in the subscript “e”); the second one, SOC_{qr} , is related to the stored charge. Although the second definition corresponds closely to the literal meaning of the SOC acronym (State-Of-Charge) and is more directly related to the equivalent concept of batteries, some researchers consider the first definition more useful, since what really matters is the energy content of the storage device.

We added to both definitions the subscript “r”, standing for *relative*. In fact, two alternative *absolute* definitions (2a) and (2b) can be used as well:

$SOC_{ea} = \frac{V_{OC}^2}{V_{max}^2}$	(2a)
$SOC_{qa} = \frac{V_{OC}}{V_{max}}$	(2b)

The *absolute* definitions have the advantage that in this case the SOC never falls below zero; when the relative definitions are adopted, this can happen in special cases, since V_{min} is just a rough indication and supercapacitor's voltage normally can decrease below V_{min} by limited amounts without any damage.

However, *absolute* definitions have the disadvantage that in the normal operation of supercapacitors the SOC range is not (0÷1) but (SOC_{min} ÷1). If, for instance, $V_{min}=V_{max}/2$, SOC_{ea} must be in the range 0.25÷1 and SOC_{qa} in the range 0.5÷1. This assumption comes from the fact that the typical voltage window considered for SCs is between $V_{max}/2$ and V_{max} . At equal power request, lower values of voltage would result in very high

currents, unacceptable for the considered device or however corresponding to intolerable losses. At equal current request, lower values of voltage would instead correspond to negligible power flows.

All the definitions reported above can be collectively referred to as follows:

$SOC = f(V_{oc})$	(3)
-------------------	-----

Between the above mentioned alternatives, in this paper the definition of SOC_{qa} has been adopted. Therefore, in the following SOC stands always for SOC_{qa} and its value is always between 0.5 and 1.

2.3 *Experimental evaluation of parameters*

After the formulation of the model, based on the single branch configuration of Figure 2 with a number of R - C blocks between $n=0$ and $n=2$, an experimental test able to evaluate the dynamic response of the model and the values of the elements R_0 , R_i , C_i , (i between 1 and n) at different SOC's has been performed.

Experimental setup is composed by a charging system driven by a 60V-250A Ametek[®] programmable DC power supply (Model SPS60X250-K02D). Discharging system is instead a 60V-500A Zentro-Elektrik[®] Electronic Load (Model EL6000). The two systems can be fully remote controlled via a GPIB standard interface, through a software developed in LabView[®]. For what concerns the measurement system, the current is measured using a shunt, class 0.5 and full scale 150 A; the voltage and the current have been acquired through a DAQ device (Model NI 9219), with a declared accuracy of 0.3% of reading. The device under test is located in a climatic chamber Binder[®] MK53, characterized by a temperature range -40°C to 180°C. All the tests have been executed with the climate chamber set at 22°C. The main rated characteristics of the supercapacitor cell under test are shown in Table 1.

Table 1: Characteristics of the SC cell

Nominal capacitance (F)	3000
Maximum voltage (V)	2.85
Nominal voltage (V)	2.7
Max continuous current (A) ΔT 15°C	130
Max continuous current (A) ΔT 40°C	210
Max peak current (A)	2000
Internal resistance (m Ω)	0.29
Leakage current ¹ (mA)	5.2
Mass (kg)	0.5

The test performed, called *Multiple Step Test* (MST), is shown in Figure 3.

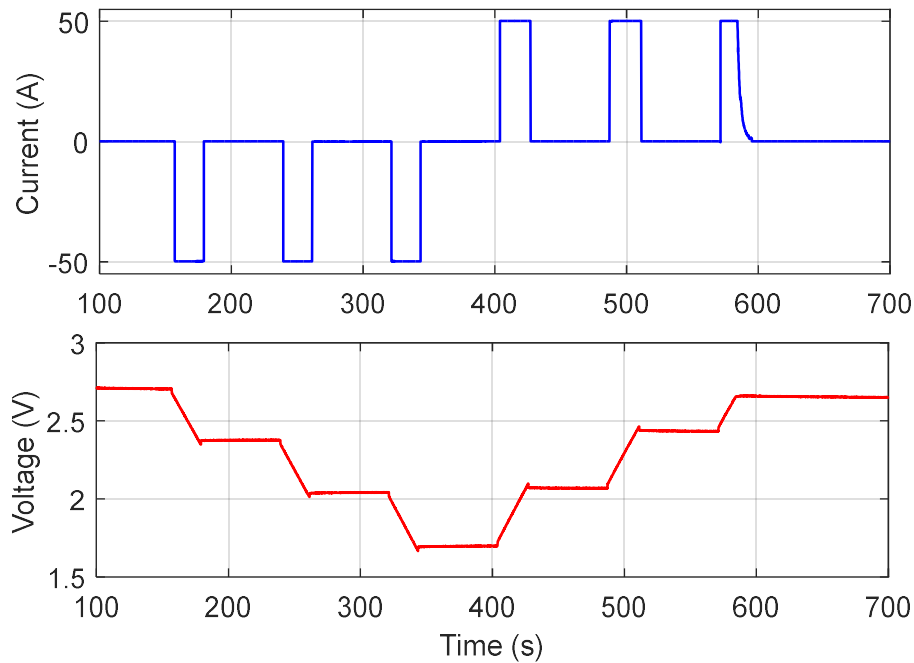


Figure 3: Current and voltage profile measured during MST

Although the values of the SC cell parameters are in general functions of the SOC and of the cell internal temperature, acceptable results can be obtained also without taking into account this dependence. This approach has been followed in this paper.

Under this assumption, the SC cell was first completely charged and then, as shown in Figure 3, subjected to three discharge pulses, interspersed by one minute rest phases, and the cell discharged. Then the cell was charged using three other charge pulses, interspersed by one-minute rest phases, until the cell was completely charged. How visible, last step shows a different slope compared to the others. In fact, a final

¹ After 72 hours at nominal voltage, initial leakage current can be higher

constant-voltage charging phase with decreasing current is observed, when the maximum admitted voltage value is reached.

Starting from the MST results, using numerical identification algorithms able to minimise the error between actual and simulated voltage profile, it is possible to evaluate the OCV as a function of SOC, as well as the trend of all the other numerical values of the circuit parameter shown in Figure 2. The error function chosen is:

$$\mathcal{E} = \min \left\{ \sum_{k=1}^K \sqrt{(v_{k,actual} - v_{k,model})^2} \right\} \quad (4)$$

where $k=1, 2, \dots, K$ are the individual values at equidistant times t_1, t_2, t_K . Figure 4 shows a comparison between experimental and simulated voltage at the end of the discharge pulse, at SOC=76%. The voltage response of the considered battery model to the same current depends on the number n of $R-C$ block, and on the numerical values of all parameters that have been determined.

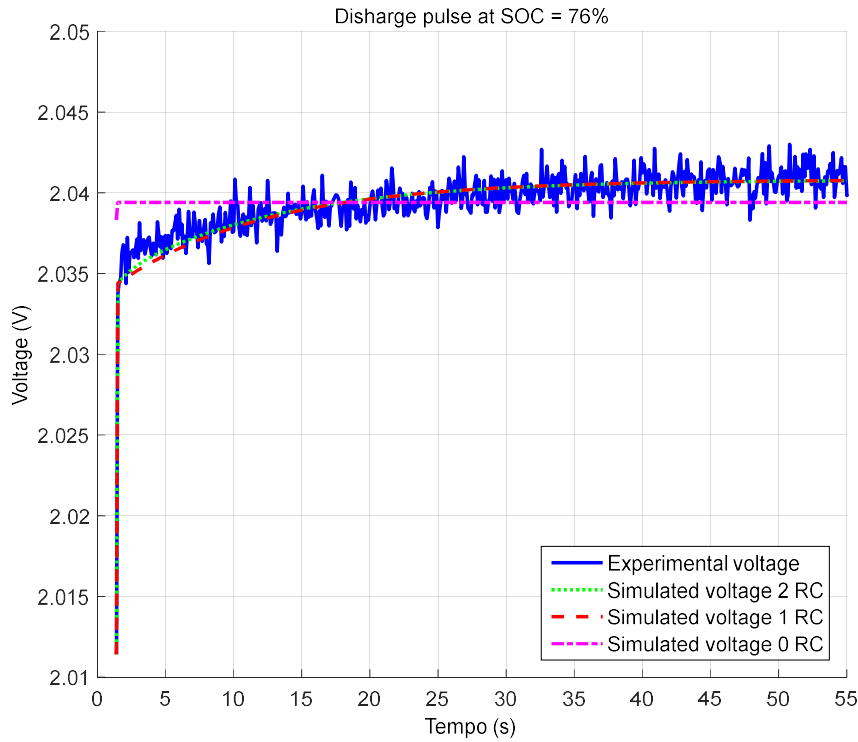


Figure 4: Comparison between experimental and simulated results in case of 0 $R-C$, 1 $R-C$ and 2 $R-C$

The comparison demonstrates that the configurations with one or two R-C blocks have rather acceptable results, while the one without R-C blocks causes a clear inaccuracy. To avoid complexity and maintaining acceptable results, the configuration with one R-C block has been then selected.

It could be argued that, at a given SOC, during charge and discharge the parameters show slightly different values. This duality cannot be dealt by simply adopting different values when the terminal current is positive or negative, because in case of a current with continuously variable sign the model precision would be very low, since the voltage would experience unreal steps at each change of the current sign.

However, acceptable results can be obtained using V_{OC} during both charge and discharge, while using intermediate values for the other parameters. These intermediate values can be evaluated simply as the arithmetic mean between those obtainable during end-of-discharge and end-of-charge identification process, or by minimising the global error, considering both end-of-discharge and end-of-charge transients. The two techniques have revealed to produce quite equivalent results; therefore the choice can be done considering practical issues related to the automatic determination of the numerical values from experimental tests. In fact, since it is expected that a periodical update of these values is required to follow the supercapacitor's aging during its life, to identify the numerical values of the model parameters it is recommended to use techniques as easily automatable as possible.

The determination of the parameters has been finally carried out at different values of SOC by using the error minimisation technique (4). The results obtained are summarised in Table 2.

Table 2: Identification of model parameters as function of SOC

SOC	V_{OC} (V)	R_0 (m Ω)	R_1 (m Ω)	R_1C_1 (s)
0.52	1.43	0.51	0.11	4.2
0.76	2.04	0.50	0.10	11
1	2.85	0.48	0.09	16

These results are such that a linear dependence of R_0 , R_1 and R_1C_1 on SOC can be assumed, or they could be even considered constant, without any dependence on SOC. Using these parameters, a comparison between simulated and experimental results can be easily made. This is for instance shown in Figure 5, considering the behaviour of the cell in response to the current profile presented in the upper part of Figure 3

(Multiple-step test). As visible for the considered portion, the model using linearly variable or constant parameters equally matches the experimental profile.

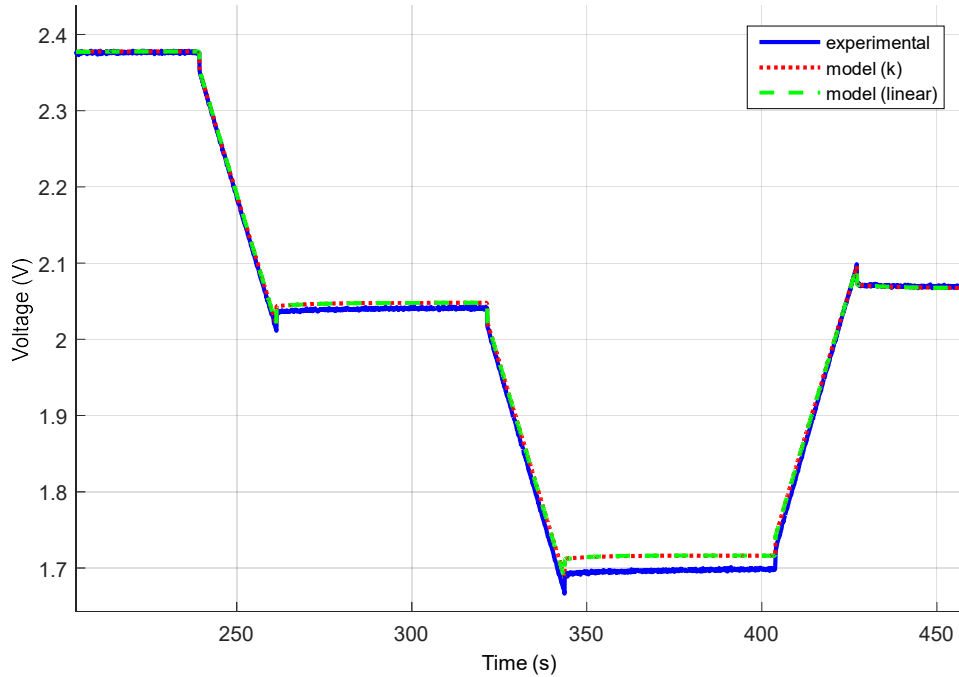


Figure 5: Experimental and simulated voltage during MST, linear dependence from SOC or constant parameters

As already noted, tests have been executed at room temperature. Several studies show how model parameters may be affected also from temperature variation [30] [31]. Implementing parameters variations over temperature is out of the scope of this paper, focused on SOC evaluation technique rather than on a deep investigation of the SC model. However, possible parameter variations induced by the temperature and calibrated as described in [30] [31] have been also tested into the model, in order to assess the robustness of the SOC estimation procedure as explained at the end of section 4.

3 SOC estimation

3.1 The SOC estimation problem

As already mentioned, one of the most common techniques to estimate the SOC is called OCV-SOC correlation. This technique consists in performing a simple Ampere-hour counting, with the addition of a voltage-based compensation. This compensation is very important to avoid that the accumulation of

measuring and computing errors over time causes large errors on the calculated SOC, as shown also in [32]. Ampere-hour counting implies continuously measuring the cell current $i(t)$, and computing the integral of it, evaluating the charge Q . In case the measuring process was unaffected by errors, according to (2b) the supercapacitor's SOC would be:

$$SOC = \frac{Q}{Q_{max}} = \frac{\int i(t)dt}{CV_{max}} = \frac{V_{OC}}{V_{max}} \quad (5)$$

It is rather apparent that pure Ampere-hour counting cannot provide a SOC measure that is valid over time, since in real operation the current measure is affected by measuring errors that would be integrated over time, drifting the SOC value. In addition, further errors are caused by numerical operations like integration. Compensation of the accumulated errors can be made when the cell's current has remained null for a time adequate to damp transients, therefore the voltage at cell's terminals can be assumed to be equal to the OCV. It is indeed of interest to estimate the maximum time interval between which two OCV measures must be taken, to avoid excessive errors on SOC produced by the Ampere-hour counting technique. To do this analysis, the symbols shown in Table 3 have been used.

Table 3: Symbols to evaluate accumulated error on SOC and relative description

Symbol	Description	Example value
I_{max}	Maximum current the sensor can measure	2000 A
ε_i	the maximum error the current sensor can make, as a ratio to I_{max}	0.01
ε_Q	maximum error on the charge exiting the cell, as obtained by numerical integration of the measured current	to be determined
ε_s	maximum allowed error on SOC estimate, before an OCV-SOC correction is needed	0.10

To evaluate the error induced on ε_Q by the errors on current measure and subsequent numerical integration, it can be assumed that:

- time is measured with a precision that is much higher than that of current, and therefore errors on the measure of time can be neglected.
- errors in evaluation of the integral of current as a consequence of the numerical integration formulas are negligible as well.

Both assumptions are reasonable, because time is actually measured very well with cheap instrumentation, and numerical integration can be very precise at a very low cost using the computation power of modern microcontrollers with floating-point units. Under these assumptions:

$$\varepsilon_Q = \varepsilon_i I_{max} \Delta t \quad (6)$$

$$\varepsilon_S = \frac{\varepsilon_Q}{Q_{max}} = \frac{\varepsilon_Q}{V_{max} C} = \varepsilon_i \frac{I_{max}}{V_{max} C} \Delta t \quad (7)$$

Assuming that time can be measured with unlimited precision, equation (6) allows eliminating ε_Q from equation (7). This latter can be then used to evaluate the maximum time interval between two consecutive measures to limit the error to ε_s , assuming the instrumentation maximum error ε_i to be known. Considering the numerical values shown as example in Table 3 and assuming $I_{max}=2000$ A, $V_{max}=2.85$ V, $C=3000$ F, from equation (7) we obtain $\Delta t=43$ s.

This is a very short time, since imposing to have zero current for a time of 1-2 s (for waiting the voltage to be stabilised) every 43 s or less, is a demanding requisite.

It would be much better if a different technique, allowing SOC to be correctly evaluated without the need of having some time intervals in which the supercapacitor current is continuously null. This is what is done by the algorithm described in the following section.

3.2 *The proposed Luenberger SOC estimation algorithm*

The principle of Luenberger-style SOC evaluation is still based on evaluating the extracted charge by integrating the battery current and correcting the results. However, unlike the previous technique, the Luenberger state estimator allows performing this correction continuously, as the actual and predicted battery voltages are compared to each other and the resulting error activates a feedback on the charge computed, requiring low computational costs as in the case described in [15]. The idea is to test how this technique works also on a supercapacitor, giving rise to the scheme shown in Figure 6.

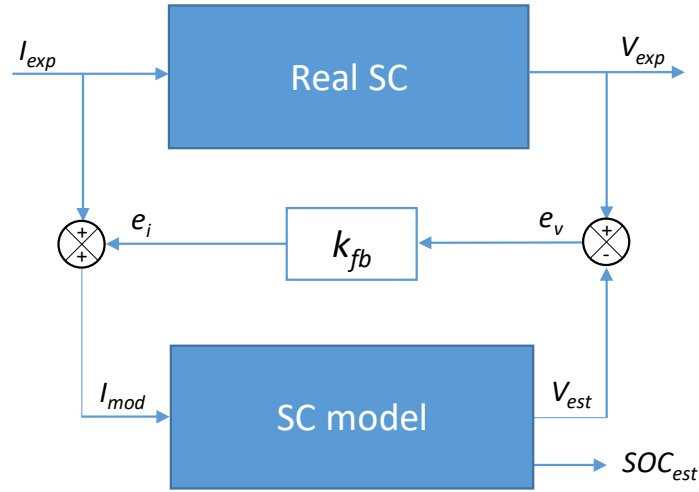


Figure 6: The Luenberger SOC estimation technique applied to a supercapacitor cell

The block named “Real SC” represent the real existing device, subjected to the applied charging/discharging current I_{exp} , while V_{exp} is the actual SC voltage. The block named "SC model" contains the model shown in Figure 2. Therefore, it receives the current I_{mod} provided by the upper loop and calculates V_{est} , i.e. the estimated terminal voltage, and consequently the SOC_{est} , the latter as an algebraic function of V_{OC} according to (2b). The estimation mechanism is as follows. Let us consider an initial condition in which the estimated voltage V_{est} is equal to the actual supercapacitor voltage V_{exp} ; in this condition the voltage error e_v and the current error e_i are zero. The supercapacitor model receives as an input the model current I_{mod} identically equal to I_{exp} .

Naturally, because of measuring errors, model uncertainties and numerical computation errors, some difference between V_{est} and V_{exp} appears. This originates a voltage error, then a current error. In this case the current value provided by the model will be:

$$I_{mod} = I_{exp} + k_{fb} e_v = I_{exp} + k_{fb} (V_{exp} - V_{est}) \quad (8)$$

The presence of the signal e_i tends to correct the errors on V_{est} and to keep well aligned V_{est} with V_{exp} . When this happens, the model is reproducing well the actual supercapacitor behaviour, and therefore the model estimation of SOC_{est} is a good approximation of the supercapacitor SOC.

It is important to fine-tune the feedback constant k_{fb} : higher values give higher corrections. The best operation is when the supercapacitor model well reproduces the real behaviour of the supercapacitor and the

measuring errors are small. In this case, small values of the feedback constant are acceptable. Typically, k_{fb} is in the order of $1\div 10$ A/V.

4 Results

4.1 Laboratory tests

The quality of the SOC estimation of the SC cell was tested based on the reference cycle shown in Figure 7. It was conceived inside the HCV Project [33] to represent the real usage of an equivalent SC module installed on-board hybrid vehicles. As explained in [8], wheel power varies linearly with speed and this profile remains unchanged moving from mechanical wheels to the electric drive. Then, using a common energy management strategy, the primary converter delivers the average power requested from propulsion, while the storage system delivers or absorbs the ripple around that average. Additionally, the selected profile is also charge balanced, to allow sufficiently long tests without the need to stop due to capacitor emptying or depletion.

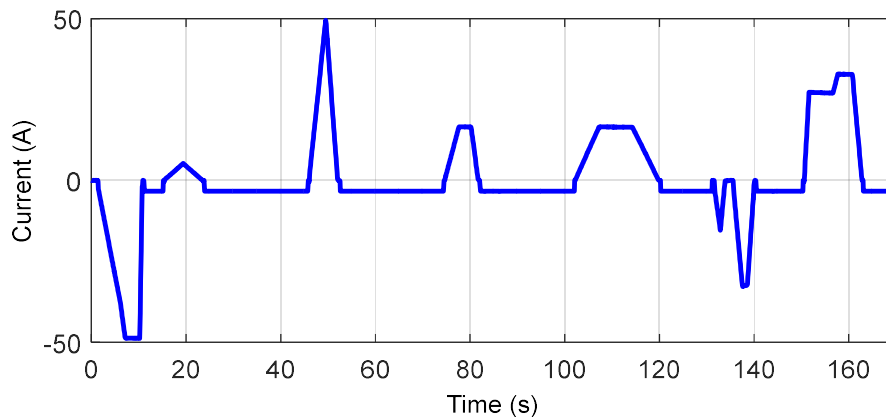


**Figure 7: Reference cycle (current vs time)
for the SC under test**

The reference cycle has been used in two main testing conditions: test 1, which consists in subjecting the cell to 48 repetitions of the reference cycle shown in Figure 7. Test 2, which consists of a long rest phase of 10 hours to evaluate the SC charge redistribution and self-discharge, after a first series of 48 reference cycles and before an additional series of other 48 reference cycles.

4.2 SOC estimation

SOC estimation has been made according to the technique depicted in Figure 6. Verification of the quality of the proposed SOC estimation procedure has been made in three steps:

- the quality of the SC model, whose parameters have been checked by subjecting the model to the actual cell current and verifying the matching of estimated and actual SC voltage;
- the quality of the Luenberger style technique, that has been implemented and verified;
- the long-term effects, due to long periods of inactivity (e.g. during nights), have been evaluated.

In all the considered steps, the model shown in Figure 2 was used, in which one single R-C block is assumed and whose parameters are shown in Table 2.

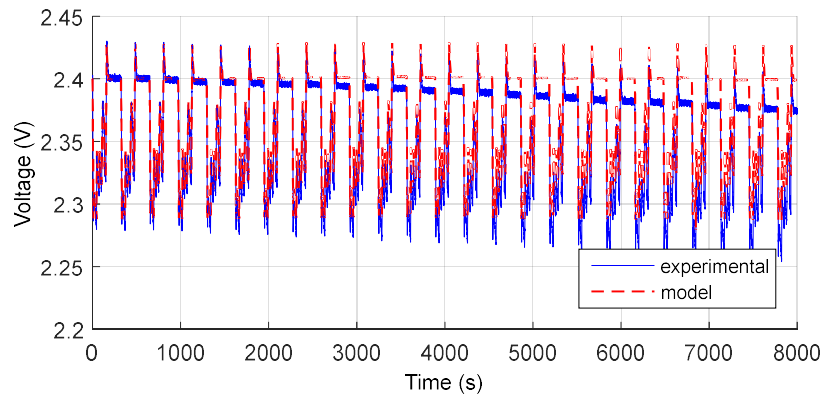
In the first step, the quality of the model has been first checked by submitting the test current to the model and comparing model's and experimental voltage. The result is displayed in the upper part of Figure 8: the quality of the model is acceptable, as for the MST test shown in Figure 3, but the global trend indicates, as expected, that some voltage drift occurs over time. As noticeable, the voltage changes within a limited range. This is effectively representative of the real usage in power-oriented applications [34], in which the storage is requested to deliver or adsorb very high currents in a very short time, corresponding to a rather small energy content.

The voltage drift is expected to be corrected by the feedback algorithm proposed in Figure 6, and used in the second step. The algorithm was run with different values for the feedback constant: the final choice has been made using $k_{fb}=10$ A/V, which allows the error to be totally offset, as shown in the middle part of Figure 8.

The third step refers to the long term stability, i.e. the ability of the proposed algorithm to provide good estimations of SOC over long periods of time. Although in the case of supercapacitors this can be considered a smaller issue since not involving their normal operation, during rest phases lasting several hours SCs show non-negligible voltage drift, due to both charge redistribution and self-discharge. The combination of these two aspects is also described in the literature [35] [36] [37].

No special problems are expected to occur in the long term with the proposed SOC estimation algorithm, since during rest phases OCV is equal to the measured voltage, and therefore actual OCV is a direct consequence of the measured voltage according to the SOC definition itself (5). Therefore, at the end of the rest period a valid SOC estimation is immediately available as the ratio of V_{OC} and V_{max} , according to (2b). This means that if the SOC estimator is left in operation during long rests, it remains aligned with the real SOC.

In case the SOC estimator is instead stopped during rest phases, for instance to avoid drawing the energy during nights, it is recommended to restart the algorithm before the SC starts drawing or absorbing current, so as to measure V_{OC} and update SOC. Even if this initial SOC update based only on V_{OC} is not performed, the algorithm's feedback operation rapidly updates the SOC value. This is shown in the bottom part of Figure 8 that explains how the algorithm is able to recover an initial SOC error using only the k_{fb} -based feedback. To do this, the transient of test 1, already shown in the middle part of Figure 8, is simulated considering an initial 1% SOC error. It is roughly equivalent to the error that would be induced by the rest phase of 10 hours of test 2, which shows a total voltage reduction of 27 mV (1% of the nominal voltage of the SC). The bottom part of Figure 8 is also obtained using k_{fb} equal to 10 A/V and clearly shows that the 1% error is rapidly recovered, confirming the algorithm's robustness. As noticeable, after a transient of 600 s, the V_{est} , i.e. the estimated terminal voltage, perfectly matches the actual voltage V_{exp} , according to the nomenclature depicted in Figure 6. On the right axis of Figure 8 (bottom), the voltage error between estimated V_{est} and experimental V_{exp} is also shown.



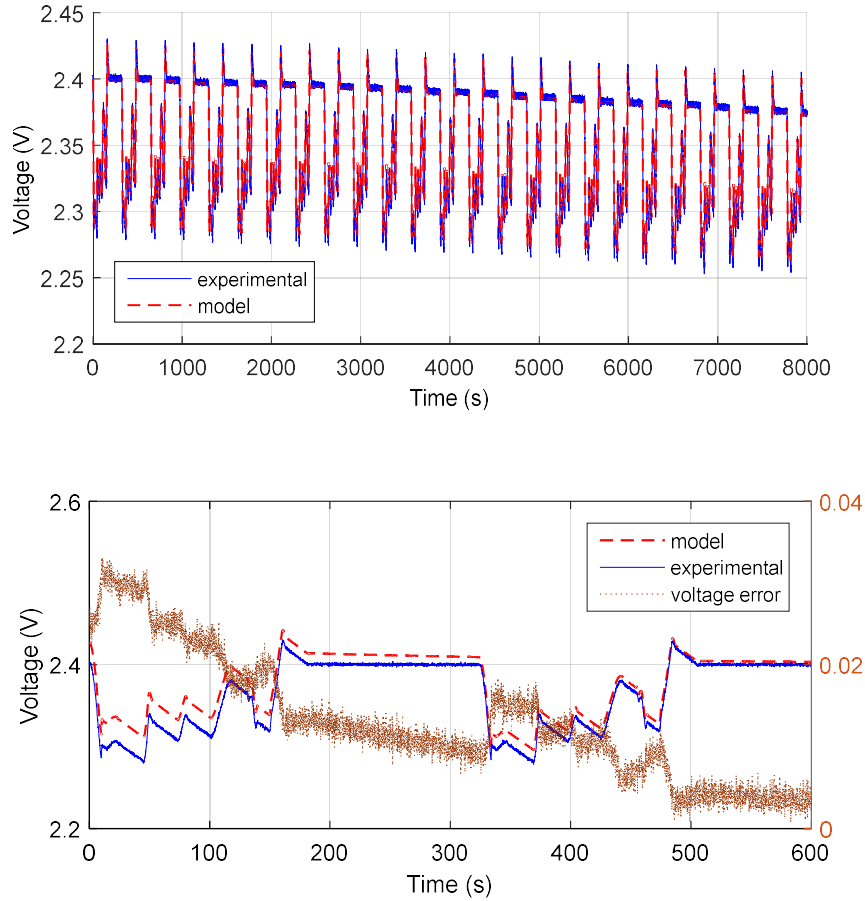


Figure 8: Simulated model (red) and experimental SC voltage (blue) without feedback algorithm (top), with feedback algorithm (middle), with feedback algorithm and initial error offset (bottom)

To further assess the robustness of the proposed technique, also taking into account possible parameter variations inducted by thermal effects [30] [31] or capacitance variations as described in [27], the algorithm was tested with a different set of parameters. Their variations were calibrated according to the cited literature, to verify if the initial error offset is rapidly corrected in analogy to what already shown in Figure 8 (bottom). More in detail, the internal resistance was changed by 10% as suggested by the extreme case of temperature dependency shown in [31], while the capacitance was modified by 20% assuming a strong dependence on voltage as discussed in [27]. We obtained that the time in which the drift is recovered was substantially unaltered, without any need to adapt k_{fb} . This gave further confidence in the robustness of the proposed technique.

5 Conclusions

This paper proposes and discusses a technique that is able to accurately measure the SOC of supercapacitors whose state of charge cannot be effectively evaluated using Ampere-counting and OCV-SOC correlation. This technique, originally conceived for batteries, has shown to be adequate also to evaluate SOC of supercapacitors subjected to high variable charging-discharging currents.

A suitable mathematical model was developed. Different configurations have been considered, analyzing the model complexity and the accuracy of results. Final choice was using one single R-C block.

Model numerical values were calibrated based on experimental results. Different parameter techniques have been tested, showing how constant or linearly variable parameters allow to correctly matching the experimental voltage profile.

A Luenberger state estimator has been proposed, described and validated. It completely avoids drifts on the measured SOC and allows fast recovery of initial errors, using both current and voltage measurements. The tuning of the algorithm parameters, as shown, is extremely fast and easy to perform.

Acknowledgements

The research leading to these results has received funding from the European Union Seventh Framework Programme (FP7/2007-2013) under grant agreement no 234019 for the Hybrid Commercial Vehicle (HCV) Project.

References

- [1] D. Poli, A. di Donato, G. Lutzemberger, “Experiences in Modeling and simulation of hydrogen fuel-cell based propulsion systems”, SAE Technical Paper 2009-24-0084, 2009.
- [2] T. Huria, G. Lutzemberger, G. Pede, G. Sanna, “Systematic development of series-hybrid bus through modelling”, Vehicle Power and Propulsion Conference (VPPC), 2010 IEEE, 1-3 Sept. 2010, Lille.
- [3] M. Li, H. Xu et alii, “The structure and control method of hybrid power source for electric vehicle”, Energy, 112 (2016), pp. 1273-1285.

- [4] S. Barsali, P. Bolognesi, M. Ceraolo, M. Funaioli, G. Lutzemberger, “Cyber-Physical Modelling of Railroad Vehicle System using Modelica Simulation Language”, Railways 2014, 8-11 Apr. 2014, Ajaccio, Corsica.
- [5] M. Ceraolo, M. Funaioli, G. Lutzemberger, M. Pasquali, D. Poli, L. Sani, “Electrical Storage for the Enhancement of Energy and Cost Efficiency of Urban Railroad Systems”, Railways 2014, 8-11 Apr. 2014, Ajaccio, Corsica.
- [6] V. Herrera, A. Milo et alii, “Adaptive energy management strategy and optimal sizing applied on a battery-supercapacitor based tramway”, Applied Energy, 169 (2016), 831-845.
- [7] M. Ceraolo, S. Barsali, G. Lutzemberger, M. Marracci, “Comparison of SC and high-power batteries for use in hybrid vehicles”, SAE Technical Paper 2009-24-0069, 2009.
- [8] M. Ceraolo, G. Lutzemberger, D. Poli, Aging evaluation of high power lithium cells subjected to micro-cycles, Journal of Energy Storage, 6 (2016), 116-124.
- [9] D. Yan, L. Lu, Z. Li et alii, “Durability comparison of four different types of high-power batteries in HEV and their degradation mechanism analysis”, Applied Energy, 179 (2016), 1123-1130.
- [10] D. Torregrossa, M. Paolone, Modelling of current and temperature effects on supercapacitors ageing. Part I: Review of driving phenomenology, Journal of Energy Storage, 5 (2016), 85-94.
- [11] D. Torregrossa, M. Paolone, Modelling of current and temperature effects on supercapacitors ageing. Part II: State of Health assessment, Journal of Energy Storage, 5 (2016), 95-101.
- [12] P. Straiti, F. Lufrano, Nafion® and Fumapem® polymer electrolytes for the development of advanced solid-state supercapacitors, Electrochimica Acta, 206 (2016), 432-439.
- [13] Y. Zhang, H. Yang et alii, A promising supercapacitor electrode material of CuBi₂O₄ hierarchical microspheres synthesized via a coprecipitation route, Journal of Alloys and Compounds, 684 (2016), 707-713.

- [14] A. Nadeau, M. Hassanalieragh et alii, "Energy awareness for supercapacitors using Kalman filter state-of-charge tracking", *Journal of Power Sources*, 296 (2015), 383-391.
- [15] X. Hu et alii, "Estimation of state of charge of a lithium-ion battery pack for electric vehicles using an adaptive Luenberger observer", *Energies*, 3 (2010), 1586-1603.
- [16] L. Zubieta, R. Bonert, "Characterization of double layer capacitors for power electronics applications", *Industry Applications, IEEE Transactions on*, 36 (2000), 199-205.
- [17] F. Belhachemi, S. Rael, B. Davat, "A physical based model of power electric double-layer supercapacitors", *IEEE Industry Applications Conference*, 5 (2000), 3069-3076.
- [18] R. Faranda et. Al., "A new simplified model of Double-Layer Capacitor", *Clean Electrical Power, 2007.ICCEP '07*, 706-710.
- [19] Lingling Du, "Study on supercapacitor equivalent circuit model for power electronics applications", *Power Electronics and Intelligent Transportation System International Conference on (PEITS)*, 2 (2009), 51-54.
- [20] H. Gualous, et. Al., "Experimental study of supercapacitor serial resistance and capacitance variations with temperature", *Journal of Power Sources*, 123 (2003), 86-93.
- [21] F. Rafik, et. Al., "Contribution to the sizing of supercapacitors and their applications", *First European symposium on supercapacitors and applications (ESSCAP)*, Belfort, France (2004).
- [22] E. Tironi, V. Musolino, "Supercapacitor characterization in power electronic applications: proposal of a new model", *International Conference on Clean Electrical Power* (2009), 376-382.
- [23] R. De Levie, "Electrochemical response of porous and rough electrodes", *Advances in Electrochemistry and Electrochemical Engineering*, Wiley InterScience, 6 (1967).
- [24] S. Buller et. Al., "Modeling the dynamic behavior of supercapacitors using impedance spectroscopy", *Industry Applications Conference*, 4 (2001), 2500-2504.

- [25] T. Huria, G. Ludovici, G. Lutzemberger, “State of charge estimation of high power lithium iron phosphate cells”, *Journal of Power Sources*, 249 (2014), 92-102.
- [26] M. Ceraolo, G. Lutzemberger, T. Huria: “Experimentally-Determined Models for High-Power Lithium Batteries”, SAE Technical Paper 2011-01-1365, 2011.
- [27] W. Sarwar, M. Marinescu et alii, “Electrochemical double layer capacitor electro-thermal modelling”, *Journal of Energy Storage*, 5 (2016), 10-24.
- [28] R. Giglioli, G. Zini, M. Conte, “Battery state of charge observer to improve energy management on electric storage plants”, 3rd International conference on Batteries for Utility Energy Storage, 1991, Kobe, Japan.
- [29] A. Bostrom et. Al., “Supercapacitor Energy Storage Systems for Voltage and Power Flow Stabilization”, 1st IEEE Conference on Technologies for Sustainability, 2013.
- [30] M. Frivaldsky, J. Cuntala, P. Spanik, “Simple and accurate thermal simulation model of supercapacitor suitable for development of module solutions”, *International Journal of Thermal Sciences*, 84 (2014), 34-47.
- [31] A. Berrueta, I. San Martin et alii, “Electro-thermal modelling of a supercapacitor and experimental validation”, *Journal of Power Sources*, 259 (2014), 154-165.
- [32] H.-S. Song et. Al., “A study on the dynamic SOC compensation of an ultracapacitor module for the hybrid energy storage system”, INTELEC 2009.
- [33] Official site HCV Project, <http://www.hcv-project.eu/>, last access: 16/01/2017
- [34] P. Venet, et. Al., “Modelling of the supercapacitors during self-discharge”, *EPE Journal*, 17 (2007), 6-10.
- [35] S.Barsali, M.Ceraolo, R.Giglioli, D.Poli, “Storage applications for smartgrids”, *Electric Power System Research (EPSR)*, Vol.120, March 2015, pages 109-117.

[36] J. Shen, Y. He, Z. Ma, “A systematical evaluation of polynomial based equivalent circuit model for charge redistribution dominated self-discharge process in supercapacitors”, *Journal of Power Sources*, 303 (2016), 294-304.

[37] H. Yang, Y. Zhang, “A study of supercapacitor charge redistribution in environmentally powered wireless sensor nodes”, *Journal of Power Sources*, 273 (2015), 223-236.